Highly efficient treatment of terephthalic acid wastewater by Fenton-like combined biodegradation

Weixia Liu, Ling Zhang, Qiulian Yang, Zhengwei Zhang, Yanhua Liu, Ruixin Guo, Oscar Lopez Torres, Zhengyu Yan*, Jianqiu Chen*

China Pharmaceutical University, Nanjing 210009, China, emails: yanzhengyujiang@163.com (Z. Yan), cjqer@163.com (J. Chen)

ABSTRACT

Treatment of terephthalic acid (TA) wastewater by a Fenton-like tourmaline/H_2O_2 system combined with aerobic activated sludge was investigated. In the case of pre-treatment, Fenton-like oxidation was aimed at decomposing the fractions of TA wastewater that can be quite difficult to degrade and then converting them into readily biodegradable products, which can be subsequently biologically removed. The degradation of the main target compound TA was observed when subjected to a Fenton-like process. A series of parameters for degradation efficiency were investigated, including the ratio of the concentration of tourmaline to H_2O_2 (F) tourmaline size, initial pH and temperature of the reaction. It was shown that when the value of F was 17.8, and the pH and temperature were 4.44 and 58°C, respectively, the catalyst presented an optimal TA degradation performance (94.8%) after 90 min. We analyzed the intermediates of TA, possible ring-opened products and proposed possible degradation schemes for TA in a Fenton-like system. However, the Fenton-like process was failed to remove chemical oxygen demand (COD) from the wastewater. Thus, a biodegradation process was used to further treat the effluent of the Fenton-like process. After 12 h of aerobic activated sludge process, 90% of COD was removed, and the pH value of the effluent ranged from 8 to 9. In addition, the dilution rates of the biological process were assessed for Fenton-like effluent. When the dilution rate was 1:1, biodegradation time was shortened, and efficiency was greatly enhanced. This study provided an effective treatment method for TA wastewater and provided a new idea for wastewater treatment.

Keywords: Terephthalic acid wastewater; Tourmaline; Fenton-like; Aerobic activated sludge; COD removal

1. Introduction

Terephthalic acid (TA) is widely used to manufacture polyester fibers, PET-film, medicines, dyes, synthetic perfumes and other chemical compounds. TA is one of the main organic components of purified terephthalic acid (PTA) manufacturing wastewater [1,2], considered toxic and an endocrine disruptor [2,3]. Wastewater from the manufacture of PTA includes high concentrations of acetic acid, functioning as a solvent, as a contaminant, and in addition contains benzoic acid (BA), p-toluic acid, phthalic acid, and

4-carboxybenzaldehyde [3,4]. Anaerobic biological treatment has been intensively applied to the treatment of PTA manufacturing wastewater [5]; however, studies of the removal of organic components by this method are limited. Aerobic treatment of PTA wastewater has not been considered a workable method, especially for wastewater that contains compounds such as acetate and benzoate [6,7], which affect the biodegradation of terephthalate [8]. It takes more than 10 d to initiate a treatment system and over 2 months to reach stable operation for anaerobic or aerobic treatment of PTA wastewater [9,10]. Moreover, using a two-stage activated

* Corresponding author.

sludge process alone for treating PTA wastewater can reduce effluent quality [11].

In past decades, utilizing advanced oxidation processes (AOPs) to remove pollutants from water and wastewater has become popular from the perspective of environmental governance [12,13]. AOPs include Fenton and Fenton-like process, heterogeneous and homogeneous photocatalysis, O_3 process, catalytic wet oxidation, sonochemical oxidation, electrochemical oxidation [14]. These processes are applied frequently for the degradation of pollutants such as oze dye [15,16], carbamazepine [17], tyrosol [18], and atrazine [19],. Also, the solar photo-Fenton combined with nanofiltration can reduce the environmental impacts of real wastewater [20]. During the AOP, hydroxyl radicals ($^{\bullet}OH$) are generated, and $^{\bullet}OH$ acts as a strong and non-selective oxidizer of organics, leading to more efficient treatment of wastewater. Among AOPs, Fenton-like processes applied as a pretreatment for wastewater can improve biodegradation of raw wastewater [21]. Homogeneous and heterogeneous photo-Fenton/Fenton-like processes have been widely used to treat TA or PTA wastewater [1,6,22,23]. Thiruvenkatachari et al. [24] pointed out that TA was degraded as benzoquinone, benzene, maleic acid, oxalic acid probably in UV-H_2O_2-Fe-O_3 system. Also, some by-products of TA in the photocatalytic ozonation system, such as muconic, fumaric, and oxalic acids were identified by Fuentes et al. [25]. These processes were effective means of degrading organic compounds which were non-biodegradable from TA wastewater. Moreover, the chemical oxygen demand (COD) removal efficiency of wastewater from the TA manufacturing process was high relatively [22]. However, the photocatalytic process requires an auxiliary light source and harsh conditions [1], restricting its practical use. When pretreated with photo-Fenton in which while almost total elimination of the major pollutants in PTA wastewater was achieved, part of their oxidation produced intermediates remained as refractory products, hard to further oxidize probably, efficient biodegradation of PTA wastewater requires several months from start-up to steady-state period [22]; therefore, using the photo-Fenton/Fenton-like method to treat wastewater is costly and time-consuming.

Tourmaline is a natural iron-bearing mineral, and its use to degrade organic compounds in Fenton-like reactions has been investigated [26]. The generalized tourmaline structural formula is described as $XY_3Z_6(T_6O_{18})(BO_3)_3V_3W$, the common ions (or vacancy) at each site are X = Na^+, Ca^{2+}, K^+; the Y = Fe^{2+}, Mg^{2+}, Mn^{2+}, Al^{3+}, Fe^{3+}, Li^+, Cr^{3+}; Z = Mg^{2+}, Fe^{3+}, Al^{3+}, Cr^{3+}; T = Al^{3+}, B^{3+}, Si^{4+}; B = B^{3+}; V = OH or O^{2-}; W = OH^-, F^-, O^{2-} [27]. Tourmaline can remove azo dyes [16], atrazine [19], and BPA [28] when combined with hydrogen peroxide. Tourmaline can easily be separated from wastewater to reduce secondary pollution. This paper considers a tourmaline-based Fenton-like process as a pretreatment for wastewater.

The purpose of this study is aimed at pretreating TA wastewater and boosting the efficiency of its biodegradation in an acceptable amount of time and reasonable reaction conditions, thus improving effluent water quality. To better optimize the catalytic activity and deduce the reaction mechanism in the Fenton-like process, the effects of ratio of concentration of tourmaline to H_2O_2, initial pH,

and tourmaline size were explored, and the degradation intermediates of the Fenton-like process were clarified by liquid chromatography-mass spectrometry (LC–MS). The COD removal by the aerobic activated sludge process was also investigated.

2. Materials and methods

2.1. Reagents and materials

TA (purity 99%) was supplied by Aladdin Industrial Corporation (Shanghai, China). 30% H_2O_2 was purchased from Nanjing Chemical Reagent Co., Ltd. BA was obtained from Tianjin Kermel Chemical Reagent Co., Ltd. HPLC-grade acetonitrile was provided by Concord Technology Co., Ltd. (Tianjin, China). Tourmaline was offered by Shijiazhuang Maoxiang Mineral Products Co., Ltd. The aerobic activated sludge was collected from a municipal sewage treatment plant (Nanjing, China). All other chemicals were analytical grade.

2.2. Preparation of TA wastewater and characterization of tourmaline

In this work, terephthalic acid wastewater (TAW) consisted of 60 mg/L TA, 40 mg/L BA, 4.2 g/L acetic acid, 1 g/L NaOH and hard water. The pH value was approximately 4.44.

Tourmaline was analyzed with the scanning electron microscopy (SEM, S-3400N II, Hitachi, Japan) and energy-dispersive X-ray spectroscopy (EDS), X-ray diffraction spectrum (XRD, D/MAX 2500, Rigaku Co., Japan), X-ray photoelectron spectroscopy (XPS, PHI 5000 Versa Probe, UlVAC-PHI, Inc., Japan/USA).

2.3. Fenton-like process

Experiments were conducted in a single-mouth round-bottomed flask (250 mL) equipped with a digital intelligent temperature control magnetic stirrer. For each experiment, 100 mL of TA solution or TAW was added to the flask, the liquid temperature was preserved at T ± 1°C, and the initial pH of the TAW was adjusted with H_2SO_4 solution. Tourmaline particles and H_2O_2 were dispersed into the TAW and mixed completely. For comparison, the experiments were maintained according to the procedures described above for the catalyzing system but without H_2O_2 or tourmaline. Specifically, the effects of the ratio of the concentration of tourmaline to H_2O_2 (F), tourmaline size, the initial pH of TAW and the reaction temperature on TA degradation were measured.

2.4. Aerobic activated sludge treatment process

A culture medium of aerobic activated sludge containing K_2HPO_4 (930 mg/L), $CaCl_2$ (101 mg/L), $MgSO_4$ (32.5 mg/L), NaCl (233 mg/L), urea (1,000 mg/L), beef extract (3,666 mg/L) and peptone (5,333 mg/L) was prepared in a 500 mL beaker. Aerobic activated sludge was maintained in the culture medium for one week for further use. Photomicrograph of aerobic activated sludge sample as shown in Fig. S1, the raw sludge consisted of a loose structure.

Biological experiments were performed separately for the raw TAW and effluent from the Fenton-like process. Aerobic activated sludge was washed several times using static sedimentation to remove any residual carbon, nitrogen, phosphorus or mineral nutrients. The initial concentration of the activated sludge was calculated to be 12 g/L after isometric mixing of the pretreated wastewater and the activated sludge. Aerators connected to an air pump were placed at the bottom of the system. The raw wastewater and pretreated wastewater with Fenton-like additions were subjected to biological treatment. To explore the effects of the initial load of wastewater on the biotreatment process, the wastewater was diluted with pure water. The pH value and COD of the solution were recorded regularly during the biodegradation process.

2.5. Wastewater sampling

During the Fenton-like process, samples were collected at regular intervals, filtered through 0.22 μm microfiltration membranes, mixed with *t*-butanol and then analyzed with high-performance liquid chromatography (HPLC, LC-20AT, Shimadzu). To survey the intermediates in the process of TA oxidation, the Fenton-like experiment was stopped after 40 min, and the solution was filtered through a 0.45 μm microfiltration membrane and extracted with ethyl acetate. The extract was evaporated at 40°C, redissolved in methanol, filtered through a 0.22 μm microfiltration membrane and was finally analyzed by LC–MS. During the biological process, samples were taken at fixed intervals and filtered through a 0.45 μm microfiltration membrane for measurements of COD and pH.

2.6. Analytical determinations

The TA concentration was measured at 240 nm with HPLC with a DAD detector and a C18 column. The mobile phase was a mixture of 0.3% acetic acid and acetonitrile (90:10, v/v) at a flow rate of 1 mL/min. Validation of the HPLC methods included linearity (R^2 = 0.999), recovery (97%~105%, RSD < 2%), precision (RSD < 2%), and detection limit (0.3 mg/L). An eight-point calibration curve was prepared with the reference substance TA at concentrations spanning those present in samples. Quantification of TA was performed using an external standard method.

Identification of TA degradation products was performed on an LC–MS (LCMS-2020, Shimadzu; MS conditions: electrospray ion scanning; scanning speed of 417 u/sec; drying gas temperature of 300°C; flow rate of 5 L/min; scanning range: m/z = 50 ~ 500). COD was determined by the dichromate method [29].

2.7. Kinetic analysis of TA degradation

Kinetic analyses indicated that the oxidation degradation of TA may follow the pseudo-first-order kinetics. The oxidation degradation process is described by Eqs (1) and (2):

$$-\frac{dC}{dt} = kC \tag{1}$$

$$-\ln\left(\frac{C}{C_0}\right) = k_t + b \tag{2}$$

in which k was the pseudo-first-order reaction rate constant (min^{-1}), t was the reaction time (min), C_0 was the initial concentration of TA, and C was the concentration of TA at time t. The reaction rate constant (k) can be calculated from the slope of the plot of $\ln(C_0/C)$ vs. (t).

3. Results and discussion

3.1. Fenton-like process

3.1.1. Characterization

SEM spectra of tourmaline (Fig. 1a) show the morphology, size and the main elements of tourmaline. It can be seen that the tourmaline sieved through 100 mesh is irregular pillar-shaped and relatively uniform, with a size of ~ 100 μm. According to the literature [27], the generalized tourmaline structural formula is $XY_3Z_6(T_6O_{18})(BO_3)_3V_3W$. As illustrated in Fig. 1b and c, Ca, Al, Fe, Mg, Si, and O elements was detected and no B, F, Li or Ti were detected suggesting that the X was Ca^{2+}, with Y and Z representing Fe^{2+}, Mg^{2+} and Al^{3+}. In addition, F was not detectable, so W is possibly O^{2-} or OH$^-$, indicating the presence of surface oxygen groups and hydroxyl groups.

The EDS spectrum supplied an elemental ratio (shown in Fig. 1b). This Fe-bearing tourmaline was named schorl. This is suitable for water treatment purposes, probably owing to it not containing F or Li elements, which are regarded as undesirable elements for human and environmental health [19].

XRD pattern of the Fe-tourmaline is shown in Fig. 1c. The sample matched the standard card (JCPDS 85-2185) well. The major peaks of tourmaline were observed at 2 theta values of 21.0°, 30.3°, 47.1°, 57.7° and 61.5°, which are in good accordance with those in previous studies [30,31].

XPS was employed to analyze the chemical valence states of iron on the surface of tourmaline. XPS measurements were implemented on the Fe2p peaks. Fig. 1d describes the Fe2p high-resolution XPS spectrum for two peaks of Fe2p3/2 and Fe2p1/2. Based on the spin–orbit (j–j) coupling, the Fe2p3/2 peaks were stronger and narrower than those of Fe2p1/2. The peak for Fe2p3/2 was located between 710.6 and 711.2 eV, however, no accurate matches were obtained, indicating the presence of other valence states of iron. After peak curve fitting with the peaks of Fe^{3+} (711.2 and 725.1 eV) through Gaussian symmetry, the two peaks were homologous with the characteristics of Fe^{3+}, and those at 709.1 and 723.5 eV were associated with Fe^{2+} peaks [32]. Furthermore, the other peaks at 715.5 and 719.0 eV were assigned to the satellite peaks of Fe^{2+} and Fe^{3+} [33], respectively. In addition, the satellite peak of Fe^{3+} at 719.0 eV would not exist if the Fe^{3+} and Fe^{2+} were in the form of Fe$_3$O$_4$, indicating that Fe^{3+} and Fe^{2+} were separately embedded in the tourmaline [33].

3.1.2. Optimizing the reaction parameters for TA degradation

The effects of different parameters such as F, initial pH, tourmaline particle size and temperature on the kinetic of
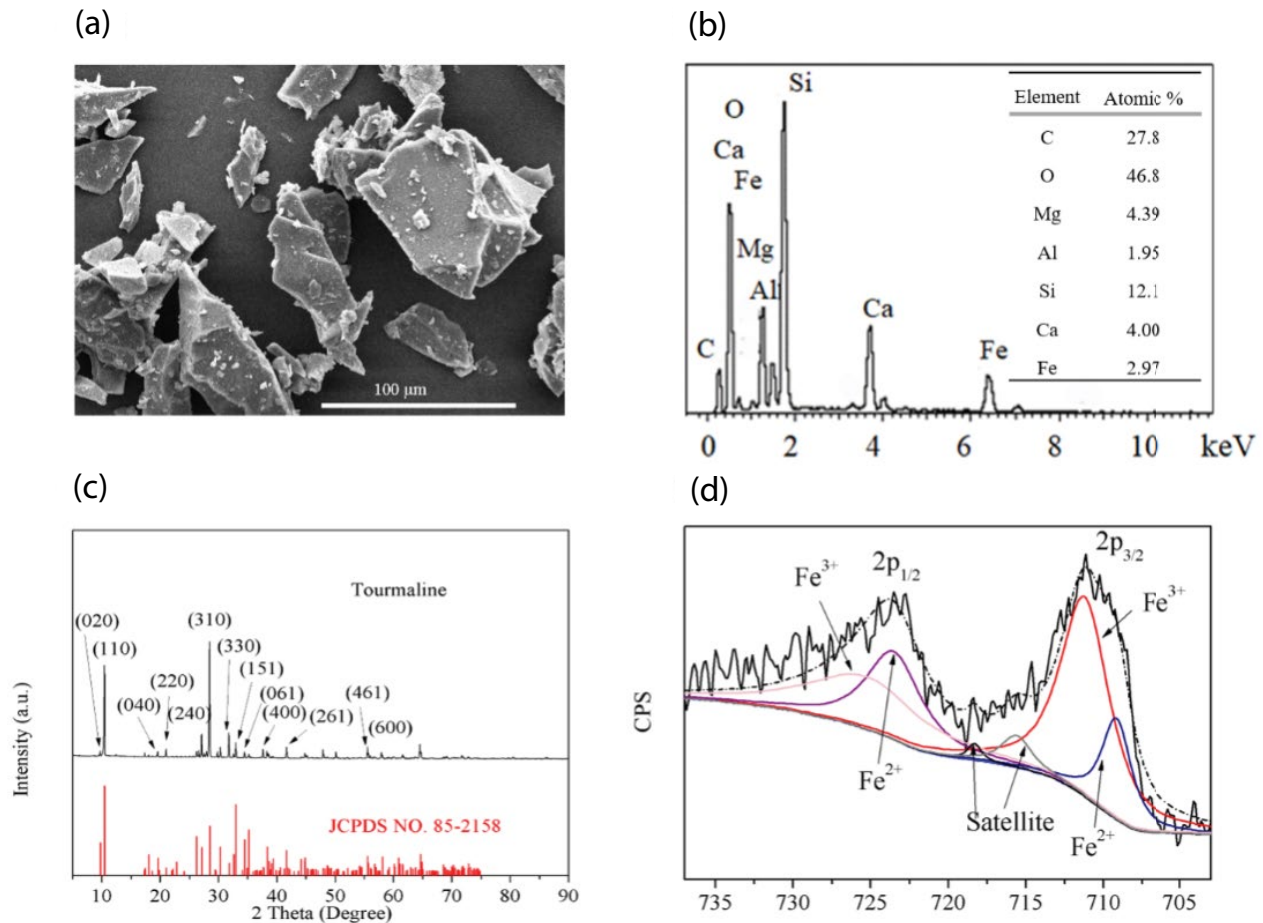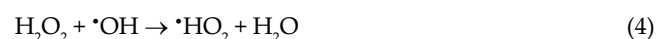
Fig. 1. Characterization of tourmaline: (a) SEM, (b) EDS, (c) XRD, and (d) XPS spectra of Fe2p.

TA degradation were assessed. The results are illustrated in Table 1. The maximum k was 2.03×10^{-2} min^{-1}.

3.1.2.1. Effects of F

To investigate the effect of F, experiments were carried out under the following conditions: 60 mg/L TA, 6.00 g/L tourmaline, with an initial pH of 4.44. As shown in Fig. S2, in the experiment where only tourmaline was added, the TA concentration was not greatly reduced, implying that TA was not absorbed or degraded. In the case of adding H_2O_2 alone, only 16.1% of the TA was decomposed. Organics can be oxidized by H_2O_2 [34] due to H_2O_2 being a relatively strong oxidant and due to the increased amount of available $^\bullet OH$ for faster catalysis of H_2O_2 at a higher temperatures [15]; however, when both tourmaline and H_2O_2 were added to the catalytic system, TA removal was enhanced obviously by increasing the concentration of H_2O_2 (shown in Fig. 2a), possibly due to the consequent acceleration in $^\bullet OH$ production. As performed in Fig. 2a, the TA degradation rate increased from 60.4% to 94.8%, while F varied from 5.60 to 17.8 after 90 min, and the optimal F was 17.8. As the F further increased and exceeded the optimum (F = 17.8, k = 0.0330 min^{-1}), there was no improvement; instead, there was a small decrease in TA removal (k = 0.0280 min^{-1})

compared to that seen at F 17.8, possibly owing to the reduction and decomposition of H_2O_2. Possible reasons include: (i) the reaction surface of tourmaline consumed a great deal of $^\bullet OH$ (see Eq. (3)) [26]; (ii) the scavenging and regeneration of H_2O_2 (as follows in Eqs. (4) and (5)) [16,35]; (iii) the reaction of $^\bullet OH$ with each other [35].

$$Fe(II) + {^\bullet OH} \rightarrow Fe(III) + OH^- \tag{3}$$

$$H_2O_2 + {^\bullet OH} \rightarrow {^\bullet HO_2} + H_2O \tag{4}$$

$${^\bullet HO_2} + {^\bullet HO_2} \rightarrow {^\bullet H_2O_2} + O_2 \tag{5}$$

3.1.2.2. Effects of tourmaline size

To survey the influence of tourmaline particle size on TA degradation, tests with different sizes of tourmaline were implemented. As shown in Fig. 2b, the TA degradation rate increased as the mesh size decreased from 80 to 100 mesh. When the size of the available tourmaline particles was further decreased by passage through 200 and 400 mesh, a noticeable decline could be seen in TA degradation. Smaller-sized tourmaline particles generally possess larger specific surface areas. When the mesh of tourmaline particles was

Table 1
Effect of different parameters on the kinetics for TA degradation

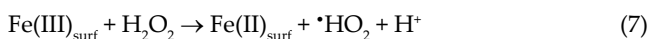| Parameters	Value	Equation	k (min^{-1})	R^2
F	5.60	$y = 0.0108x + 0.00125$	1.08×10^{-2}	0.987
	11.2	$y = 0.0174x + 0.00961$	1.74×10^{-2}	0.949
	17.8	$y = 0.0330x - 0.192$	3.30×10^{-2}	0.966
	23.4	$y = 0.0281x - 0.201$	2.81×10^{-2}	0.961
Tourmaline size (Mesh)	80	$y = 0.0283x - 0.217$	2.83×10^{-2}	0.977
	100	$y = 0.0330x - 0.192$	3.30×10^{-2}	0.966
	200	$y = 0.0260x - 0.263$	2.60×10^{-2}	0.978
	400	$y = 0.0185x + 0.251$	1.85×10^{-2}	0.978
Initial pH	4.44	$y = 0.0330x - 0.192$	3.30×10^{-2}	0.966
	5.38	$y = 0.00291x + 0.0681$	0.291×10^{-2}	0.934
	6.44	$y = 0.000943x - 0.00486$	0.0943×10^{-2}	0.996
	7.38	$y = 0.000100x + 0.00571$	0.0100×10^{-2}	0.719
Temperature (°C)	25	$y = 0.0139x - 0.0800$	1.39×10^{-2}	0.984
	58	$y = 0.0330x - 0.192$	3.30×10^{-2}	0.966
	91	$y = 0.00633x + 0.519$	0.633×10^{-2}	0.693
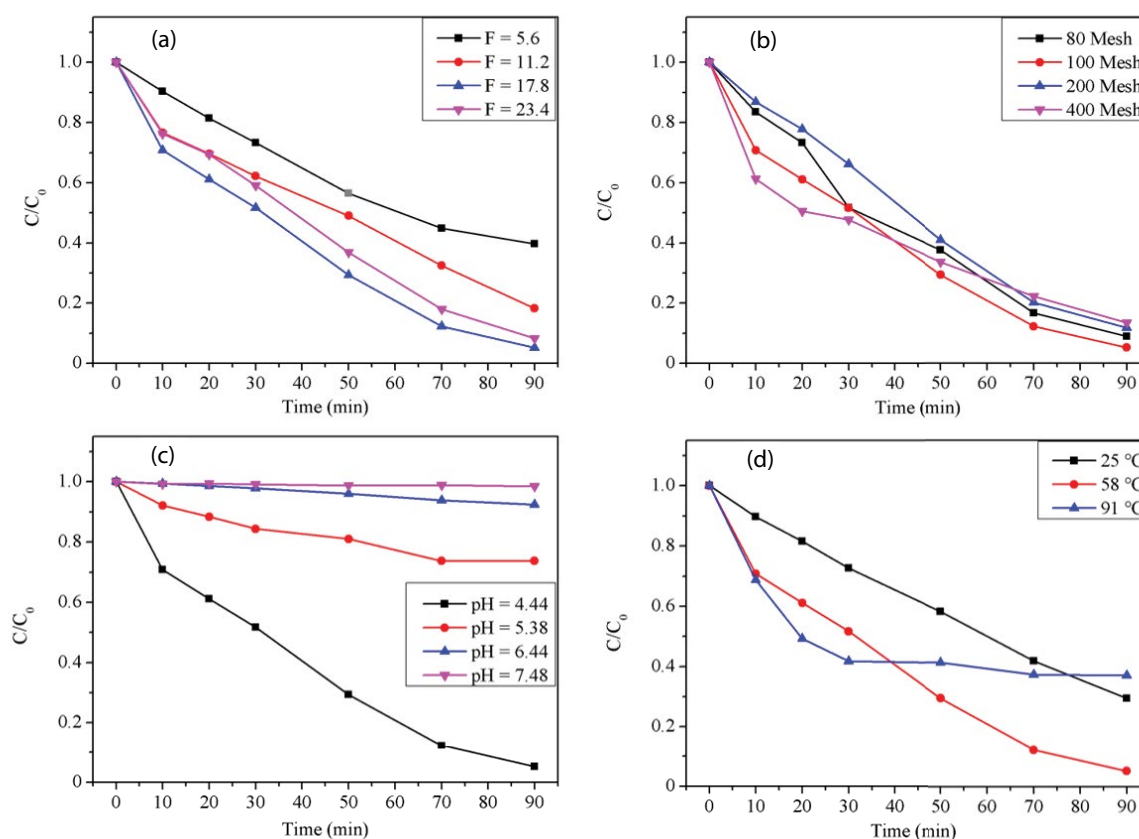
Fig. 2. Effect of different conditions on TA removal in the Fenton-like process: (a) ratio of concentration of tourmaline to H$_2$O$_2$ concentration, (b) tourmaline size, (c) initial pH, and (d) reaction temperature.

200 and 400, tourmaline possessed a large specific area, allowing more •OH to be consumed on the surface of tourmaline [36] and resulting in a decline in TA degradation. Larger-sized tourmaline particles may have less available reactive sites to enhance Fenton-like reactions [37]. The best catalytic activity was observed in these results when the size of the mesh permitting passage of tourmaline particles is 100.

3.1.2.3. Effects of initial pH

TAW is a buffer solution for acetic acid-sodium acetate. The pKa1 of TA is 3.51, and the pKa2 is 4.46 [38]. When the pH of TAW was less than 4.44, TA precipitation appeared, so all the TAW degradation experiments involving Fenton-like components were conducted at pH values greater than 4.44. The initial pH of the solution played a significant role in the iron/H_2O_2 oxidation system. As expressed by Eq. (2), k can be calculated by performing experiments under different initial pH values of TAW. Changes in the degradation rate and k under different pH conditions are depicted in Fig. 2c and Table 1 respectively. Fig. 2c clearly shows that at a pH of 4.44, the degradation of TA is much faster than at higher pH values (5.38, 6.44 and 7.48). With acidic pH values, the following reaction may occur (Eqs. (6) and (7)) [36]. The acidic environment favors degradation of TA, with optimal performance occurring at a pH of 4.44 (94.8%), while under weak acidic or neutral conditions the degradation rate decreased significantly from 27.2% to 1.5%. These results indicate higher pH values weaken the activity of TA degradation.

$$Fe(II)_{surf} + H_2O_2 \rightarrow Fe(III)_{surf} + {}^{\bullet}OH + OH^- \tag{6}$$

$$Fe(III)_{surf} + H_2O_2 \rightarrow Fe(II)_{surf} + {}^{\bullet}HO_2 + H^+ \tag{7}$$

3.1.2.4. Effects of temperature

As shown in Fig. 2d, the TA removal rate rose with increasing temperatures, from 25°C to 58°C, indicating that higher temperatures may be preferable for TA degradation. It was obvious that the treatment efficiency could be improved by increasing temperature, because higher temperatures can provide more energy to overcome the reaction activation energy [39], augmenting the reaction rate constant (shown in Table 1), thus accelerating the reaction [40]. However, a higher temperature (>58°C) decelerated TA degradation, possibly due to the decomposition of H_2O_2 into oxygen and water [41]; therefore, the optimal temperature is 58°C.

3.1.2.5. Identification of intermediates and possible schemes of TA degradation

Identification of the TA degradation intermediates was performed with LC–MS. Identified peaks are presented in Fig. 3. Each main m/z peak in the MS is assigned to a corresponding fragment structure. The ${}^{\bullet}OH$ was probably trapped by TA and attacked the ortho position of the carboxyl group [42], then TA was oxidized to TA-OH [43], which corresponded to m/z 181 as shown in Fig. 3b. Peak m/z 121 (Fig. 3d) corresponds to BA resulting from the decarboxylation of TA [44]. The main reaction between BA and hydroxyl groups is that ${}^{\bullet}OH$ directly attacks the aromatic ring, so the peak with an m/z value of 137 probably represents hydroxybenzoic acid (HBA). The characteristic maximum absorption wavelength of HBA located at 254 nm can only be detected in HPLC (not shown), so the structure of HBA was symmetrical, namely, 4-HBA, which is consistent with the literature [45].

Based on previous research [46], the main product of 4-HBA reacting with ${}^{\bullet}OH$ is 3,4-DHBA, and the corresponding peak at m/z 153 is shown in Fig. 3a. 3,4-DHBA continued to react with ${}^{\bullet}OH$ to form an isomer of trihydroxybenzoic acid (THBA) [47] with m/z value 193. Benzene was also detected with m/z value 77, probably due to the decarboxylation of BA [47]. Phenol can be produced from the decarboxylation of HBA [48] or the reaction between benzene and ${}^{\bullet}OH$ [47], so the peak at m/z 93 should be attributed to phenol. In addition, some aliphatic acid was also detected through LC–MS, as illustrated in Fig. 3a–c. The short-chain compounds may be butylene aldehyde, hexenic, open-ring products or other unknown products. Based on the above analysis, possible degradation schemes were proposed, as shown in Fig. 4.

3.2. Biological process

The COD of raw TAW was 4,380 mg/L. Under optimal conditions for the Fenton-like process, 94.8% TA was removed, the COD decreased from 4,380 to 4,200 mg/L, and the pH changed from 4.46 to 4.40. No significant change in COD could be found in the TAW, indicating that organic
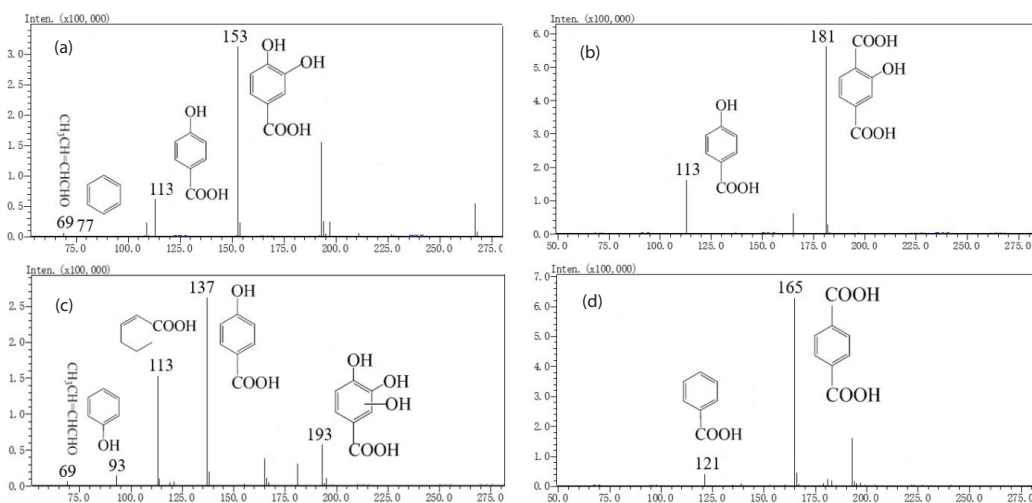

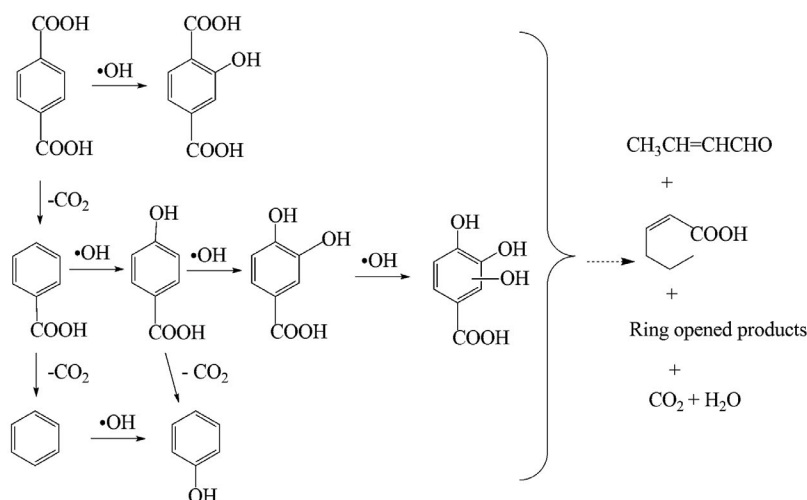Fig. 3. LC–MS spectra of TA degradation compounds.

Fig. 4. Proposed reaction schemes of TA degradation.

carbon may still be present in the effluent from the Fenton-like process; this result may be caused by the low mineralization yield. Although the COD removal of the Fenton-like process is very low, the benzene rings of TA and BA are opened to allow the generation of short-chain small molecules (shown in Fig. 4), which may be more biodegradable; therefore, the combined Fenton-like and biological methods are possibly more effective in treating TAW.

After TAW was subjected to the Fenton-like treatment at optimal conditions, the effluent was biodegraded by aerobic activated sludge. The biological process was evaluated based on COD removal and pH value. Fig. 5 shows the effects of the reaction time on the biological treatment of the raw wastewater and the effluent from the Fenton-like reaction. When aerobic activated sludge was employed to treat the effluent from the Fenton-like reaction directly, the initial COD was 4,200 mg/L, and the COD removal efficiency increased as the reaction time was prolonged from 0 to 12 h before decreasing slightly at 18 h (shown in Fig. 5a). When the reaction time was 12 h, the maximum COD removal rate was 90.1% for the effluent of pretreatment, which is attributable to the assimilation of some degradation products by microorganisms
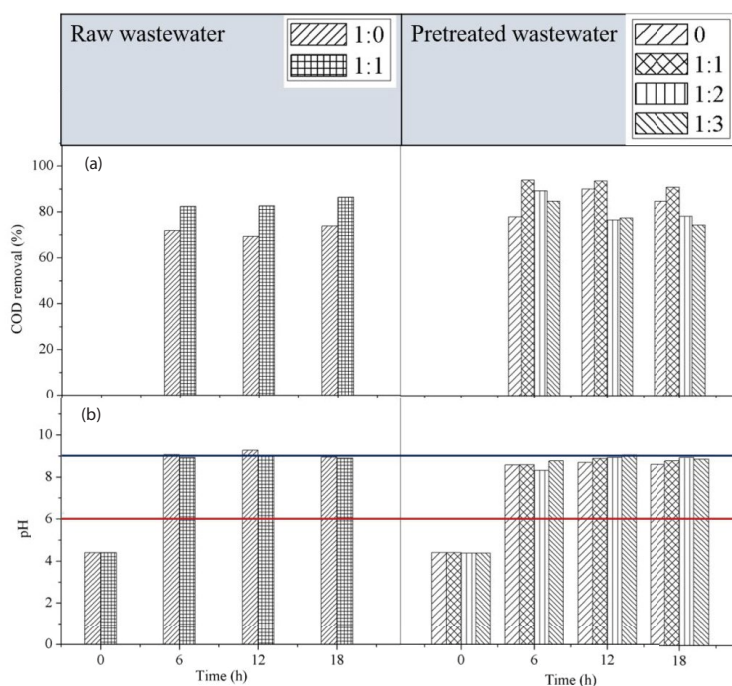

Fig. 5. COD removal and pH value of effluent after activated sludge treatment with/without Fenton-like in different dilution: (a) COD removal and (b) changing of pH value. Redline and blue lines represent the minimum pH value and maximum pH value, respectively, which meet with the national effluent discharge standard.

[49]; further, TA could not be found. In contrast, regarding the degradation of raw wastewater with high initial COD (4,380 mg/L), Fig. 5a shows that the optimal reaction time was 18 h, 71.9% COD was removed, and the TA was not completely degraded (not shown).

In addition, as shown in Fig. 5b, after the biological treatment for 12 h, the pH of effluent was 8.69 in combined treatment, while that was 9.27 in the sludge alone treatment. When the reaction time was 18 h, the pH values of the effluent of both raw and pretreated wastewater were between 8 and 9; therefore, it can be verified that Fenton-like treatment as a pretreatment process boosted the wastewater biodegradation efficiency with a COD 348 mg/L and pH 8.69.

AOPs as a pretreatment method for biological processes have been widely applied [50]. For AOPs, the complete mineralization of organic pollutants is expensive because the intermediates are more refractory to oxidation than the parent compounds. On the other hand, intermediates including short-chain organic acids can enter cells more easily [51]. Pretreatment with Fenton-like oxidation can improve the biodegradability of wastewater, and the COD of the wastewater can be greatly decreased or the BOD_5/COD ratio can be increased [52]. In this study, the COD removal rate increased possibly because the biological process was more efficient at degrading the products of the Fenton-like than that at degrading TA or BA.

After double dilution of the raw wastewater and Fenton-like effluent, the maximum COD removal rate of the raw wastewater increased 86.3% at 18 h, and that of the effluent from pretreatment reached 93.5% at 6 h. This suggests that the pretreatment with Fenton-like and lower initial COD favoured the biodegradation of wastewater. The dilution of the effluent from pretreatment ranged from 0 to 1: 3, and the initial COD value from 4,200 to 1,051 mg/L (Fig. 5b). Based on the results, the time required to reach the maximum COD removal rate was 6 h. At a dilution rate of 1:1, the COD removal rate (93.5%) was higher than the other rates, indicating a suitable dilution ratio of 1:1. The pH of the pretreated wastewater was between 8 and 9 in all cases.

4. Conclusions

Thus, coupling Fenton-like and biodegradation processes is a successful treatment to treat TA wastewater. Through the investigation of the effects of F, buffer pH and temperature, the catalytic efficiency was greatly improved in the Fenton-like process. Under the optimum condition (F of 17.8, pH of 4.44, and the temperature of 58°C), TA remove rate reaches 94.8% in the Fenton-like process after 90 min. In addition, seven intermediate products of TA at m/z 153, 181, 77, 93, 193, 121 and 137 and possible ring-opened products including short-chain carboxylic acids were detected. Furthermore, low COD removal from TA wastewater was achieved with the Fenton-like reaction. To reduce COD content in wastewater, the biological process was used to treat the effluent of the Fenton-like process. After 12 h of aerobic activated sludge process, >90% of COD was removed. Effluent water quality was improved in the pH range from 8 ~ 9 by combining the Fenton-like treatment with the aerobic activated sludge process. We believe that our work may provide a new strategy for TA wastewater treatment.

References

[1] V. Vaiano, G. Sarno, O. Sacco, D. Sannino, Degradation of terephthalic acid in a photocatalytic system able to work also at high pressure, Chem. Eng. J., 312 (2017) 10–19.

[2] Z.Y. Zhang, L.P. Ma, X.X. Zhang, W.X. Li, Y. Zhang, B. Wu, L.Y. Yang, S.P. Cheng, Genomic expression profiles in liver of mice exposed to purified terephthalic acid manufacturing wastewater, J. Hazard. Mater., 181 (2010) 1121–1126.

[3] X.X. Zhang, S.L. Sun, Y. Zhang, B. Wu, Z.Y. Zhang, B. Liu, L.Y. Yang, S.P. Cheng, Toxicity of purified terephthalic acid manufacturing wastewater on reproductive system of male mice (Mus musculus), J. Hazard. Mater., 176 (2010) 300–305.

[4] M.M. Liu, S.Q. Wang, M.K. Nobu, B.T.W. Bocher, S.A. Kaley, W.T. Liu, Impacts of biostimulation and bioaugmentation on the performance and microbial ecology in methanogenic reactors treating purified terephthalic acid wastewater, Water Res., 122 (2017) 308–316.

[5] S.S. Cheng, C.Y. Ho, J.H. Wu, Pilot study of UASB process treating PTA manufacturing wastewater, Water Sci. Technol., 36 (1997) 73–82.

[6] A. Shafaei, M. Nikazar, M. Arami, Photocatalytic degradation of terephthalic acid using titania and zinc oxide photocatalysts: comparative study, Desalination, 252 (2010) 8–16.

[7] R. Kleerebezem, J. Mortier, L.W.H. Pol, G. Lettinga, Anaerobic pre-treatment of petrochemical effluents: terephthalic acid wastewater, Water Sci. Technol., 36 (1997) 237–248.

[8] Y.S. Lee, G.B. Han, Treatment of wastewater from purified terephthalic acid (PTA) production in a two-stage anaerobic expanded granular sludge bed system, Environ. Eng. Res., 19 (2014) 355–361.

[9] K.L. Ma, X.K. Li, L.L. Bao, Influence of organic loading rate on purified terephthalic acid wastewater treatment in a temperature staged anaerobic treatment (TSAT) system: performance and metagenomic characteristics, Chemosphere, 220 (2019) 1091–1099.

[10] J.W. Liu, J. Zhou, N. Xu, A.Y. He, F.X. Xin, J.F. Ma, Y. Fang, W.N. Zhang, S.X. Liu, M. Jiang, W.L. Dong, Performance evaluation of a lab-scale moving bed biofilm reactor (MBBR) using polyethylene as support material in the treatment of wastewater contaminated with terephthalic acid, Chemosphere, 227 (2019) 117–123.

[11] G.R. Pophali, R. Khan, R.S. Dhodapkar, T. Nandy, S. Devotta, Anaerobic–aerobic treatment of purified terephthalic acid (PTA) effluent; a techno-economic alternative to two-stage aerobic process, J. Environ. Manage., 85 (2007) 1024–1033.

[12] A. Babuponnusami, K. Muthukumar, A review on Fenton and improvements to the Fenton process for wastewater treatment, J. Environ. Chem. Eng., 2 (2014) 557–572.

[13] M. Zhang, H. Dong, L. Zhao, D.X. Wang, D. Meng, A review on Fenton process for organic wastewater treatment based on optimization perspective, Sci. Total Environ., 670 (2019) 110–121.

[14] R. Dewil, D. Mantzavinos, I. Poulios, M.A. Rodrigo, New perspectives for advanced oxidation processes, J. Environ. Manage., 195 (2017) 93–99.

[15] H.Y. Xu, M. Prasad, Y. Liu, Schorl: a novel catalyst in mineral-catalyzed Fenton-like system for dyeing wastewater discoloration, J. Hazard. Mater., 165 (2009) 1186–1192.

[16] C.P. Wang, Y.W. Zhang, L. Yu, Z.Y. Zhang, H.W. Sun, Oxidative degradation of azo dyes using tourmaline, J. Hazard. Mater., 260 (2013) 851–859.

[17] L. Rizzo, T. Agovino, S. Nahim-Granados, M. Castro-Alférez, P. Fernández-Ibáñez, M.I. Polo-López, Tertiary treatment of urban wastewater by solar and UV-C driven advanced oxidation with peracetic acid: effect on contaminants of emerging concern and antibiotic resistance, Water Res., 149 (2019) 272–281.

[18] M.Y. Kilic, W.H. Abdelraheem, X. He, K. Kestioglu, D.D. Dionysiou, Photochemical treatment of tyrosol, a model phenolic compound present in olive mill wastewater, by hydroxyl and sulfate radical-based advanced oxidation processes (AOPs), J. Hazard. Mater., 367 (2019) 734–742.

[19] D. Wang, H.D. Xu, J. Ma, X.H. Lu, J.Y. Qi, S. Song, Strong promoted catalytic ozonation of atrazine at low temperature using tourmaline as catalyst: Influencing factors, reaction mechanisms and pathways, Chem. Eng. J., 354 (2018) 113–125.

[20] A. Gallego-Schmid, R.R.Z. Tarpani, S. Miralles-Cuevas, A. Cabrera-Reina, S. Malato, A. Azapagic, Environmental assessment of solar photo-Fenton processes in combination with nanofiltration for the removal of micro-contaminants from real wastewaters, Sci. Total Environ., 650 (2019) 2210–2220.

[21] X.D. Qi, Z.H. Li, Efficiency optimization of a microwave-assisted Fenton-like process for the pretreatment of chemical synthetic pharmaceutical wastewater, Desal. Wat. Treat., 57 (2016) 11756–11764.

[22] K.C. Pillai, T.O. Kwon, I.S. Moon, Degradation of wastewater from terephthalic acid manufacturing process by ozonation catalyzed with Fe^{2+}, H_2O_2 and UV light: direct versus indirect ozonation reactions, Appl. Catal., B, 91 (2009) 319–328.

[23] H.B. Yener, M. Yılmaz, Ö. Deliismail, S.F. Özkan, Ş.Ş. Helvacı, Clinoptilolite supported rutile TiO_2 composites: synthesis, characterization, and photocatalytic activity on the degradation of terephthalic acid, Sep. Purif. Technol., 173 (2017) 17–26.

[24] R. Thiruvenkatachari, T.O. Kwon, J.C. Jun, S. Balaji, M. Matheswaran, I.S. Moon, Application of several advanced oxidation processes for the destruction of terephthalic acid (TPA), J. Hazard. Mater., 142 (2007) 308–314.

[25] I. Fuentes, J.L. Rodríguez, T. Poznyak, I. Chairez, Photocatalytic ozonation of terephthalic acid: a by-product-oriented decomposition study, Environ. Sci. Pollut. Res., 21 (2014) 12241–12248.

[26] N.N. Wang, T. Zheng, G.S. Zhang, P. Wang, A review on Fenton-like processes for organic wastewater treatment, J. Environ. Chem. Eng., 4 (2016) 762–787.

[27] D.J. Henry, M. Novák, F.C. Hawthorne, A. Ertl, B.L. Dutrow, P. Uher, F. Pezzotta, Nomenclature of the tourmaline-supergroup minerals, Am. Mineral., 96 (2011) 895–913.

[28] L. Yu, C.P. Wang, X.H. Ren, H.W. Sun, Catalytic oxidative degradation of bisphenol A using an ultrasonic-assisted tourmaline-based system: influence factors and mechanism study, Chem. Eng. J., 252 (2014) 346–354.

[29] J. Yao, B. Pan, R. Shen, T. Yuan, J. Wang, Differential control of anode/cathode potentials of paired electrolysis for simultaneous removal of chemical oxygen demand and total nitrogen, Sci. Total Environ., 687 (2019) 198–205.

[30] J.P. Meng, J.S. Liang, X. Ou, Y. Ding, G. Liang, Effects of mineral tourmaline particles on the photocatalytic activity of TiO_2 thin films, J. Nanosci. Nanotechnol., 8 (2008) 1279–1283.

[31] Y.M. Hu, X. Yang, The surface organic modification of tourmaline powder by span-60 and its composite, Appl. Surf. Sci., 258 (2012) 7540–7545.

[32] A.P. Grosvenor, B.A. Kobe, M.C. Biesinger, N.S. McIntyre, Investigation of multiplet splitting of Fe2p XPS spectra and bonding in iron compounds, Surf. Interface Anal., 36 (2004) 1564–1574.

[33] T. Yamashita, P. Hayes, Analysis of XPS spectra of Fe^{2+} and Fe^{3+} ions in oxide materials, Appl. Surf. Sci., 254 (2008) 2441–2449.

[34] Y.Y. Chen, Y.L. Ma, J. Yang, L.Q. Wang, J.M. Lv, C.J. Ren, Aqueous tetracycline degradation by H_2O_2 alone: removal and transformation pathway, Chem. Eng. J., 307 (2017) 15–23.

[35] J. De Laat, H. Gallard, Catalytic decomposition of hydrogen peroxide by Fe(III) in homogeneous aqueous solution: mechanism and kinetic modeling, Environ. Sci. Technol., 33 (1999) 2726–2732.

[36] K. Rusevova, F.D. Kopinke, A. Georgi, Nano-sized magnetic iron oxides as catalysts for heterogeneous Fenton-like reactions-Influence of Fe(II)/Fe(III) ratio on catalytic performance, J. Hazard. Mater., 241 (2012) 433–440.

[37] Y.H. Zhang, J. Shi, Z.W. Xu, Y. Chen, D.M. Song, Degradation of tetracycline in a schorl/H_2O_2 system: Proposed mechanism and intermediates, Chemosphere, 202 (2018) 661–668.

[38] H. Macarie, A. Noyola, J.P. Guyot, Anaerobic treatment of a petrochemical wastewater from a terephthalic acid plant, Water Sci. Technol., 25 (1992) 223–235.

[39] S. Hashemian, Fenton-like oxidation of malachite green solutions: kinetic and thermodynamic study, J. Chem., (2013) 7p, https://doi.org/10.1155/2013/809318.

[40] T.A. Kurniawan, W.H. Lo, Removal of refractory compounds from stabilized landfill leachate using an integrated H_2O_2 oxidation and granular activated carbon (GAC) adsorption treatment, Water Res., 43 (2009) 4079–4091.

[41] C. Catrinescu, C. Teodosiu, M. Macoveanu, J. Miehe-Brendlé, R.L. Dred, Catalytic wet peroxide oxidation of phenol over Fe-exchanged pillared beidellite, Water Res., 37 (2003) 1154–1160.

[42] M. Saran, K.H. Summer, Assaying for hydroxyl radicals: hydroxylated terephthalate is a superior fluorescence marker than hydroxylated benzoate, Free Radical Res., 31 (1999) 429–436.

[43] T. Charbouillot, M. Brigante, G. Mailhot, P.R. Maddigapu, C. Minero, D. Vione, Performance and selectivity of the terephthalic acid probe for OH as a function of temperature, pH and composition of atmospherically relevant aqueous media, J. Photochem. Photobiol., A, 222 (2011) 70–76.

[44] Y. Zhuang, B.B. Jiang, J.D. Wang, Y.R. Yang, Catalytic decarboxylation mechanism of terephthalic acid to benzene over ZnO catalyst, Acta Petrolei Sinica (Petroleum Procession Section), 31 (2015) 698–704.

[45] K. Bubacz, E. Kusiak-Nejman, B. Tryba, A.W. Morawski, Investigation of OH radicals formation on the surface of TiO_2/N photocatalyst at the presence of terephthalic acid solution. Estimation of optimal conditions, J. Photochem. Photobiol. A, 261 (2013) 7–11.

[46] R. Ojani, A. Khanmohammadi, J.B. Raoof, Photoelectrocatalytic degradation of p-hydroxybenzoic acid at the surface of a titanium/titanium dioxide nanotube array electrode using electrochemical monitoring, Mater. Sci. Semicond. Process., 31 (2015) 651–657.

[47] R. Oliveira, D. Geraldo, F. Bento, Electrogenerated HO radical reactions: the role of competing reactions on the degradation kinetics of hydroxy-containing aromatic compounds, Electrochim. Acta, 135 (2014) 19–26.

[48] V.S. Mohite, M.A. Mahadik, S.S. Kumbhar, Y.M. Hunge, J.H. Kim, A.V. Moholkar, K.Y. Rajpure, C.H. Bhosale, Photoelectrocatalytic degradation of benzoic acid using Au doped TiO_2 thin films, J. Photochem. Photobiol. B, 142 (2015) 204–211.

[49] J.M. Fontmorin, F. Fourcade, F. Geneste, S. Floner, S. Huguet, A. Amrane, Combined process for 2, 4-Dichlorophenoxyacetic acid treatment-coupling of an electrochemical system with a biological treatment, Biochem. Eng. J., 70 (2013) 17–22.

[50] D. Mantzavinos, E. Psillakis, Enhancement of biodegradability of industrial wastewaters by chemical oxidation pre-treatment, J. Chem. Technol. Biotechnol., 79 (2004) 431–454.

[51] L. Rizzo, Bioassays as a tool for evaluating advanced oxidation processes in water and wastewater treatment, Water Res., 45 (2011) 4311–4340.

[52] A.R. Prazeres, F. Carvalho, J. Rivas, Fenton-like application to pretreated cheese whey wastewater, J. Environ. Manage., 129 (2013) 199–205.
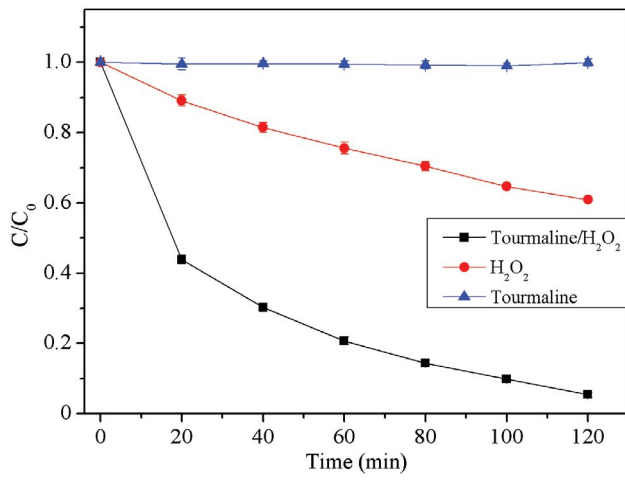
Supporting information

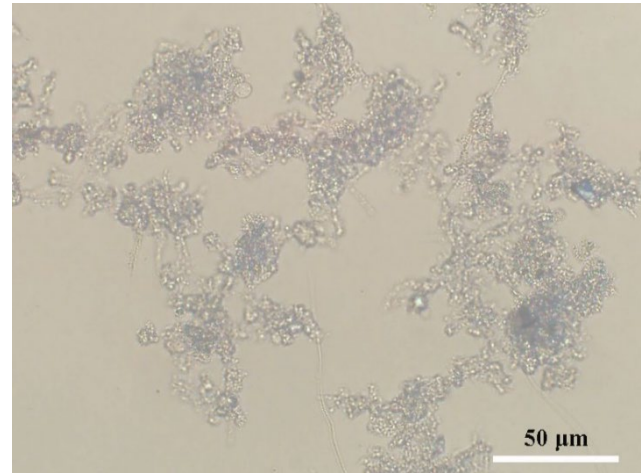Fig. S1. Degradation of TA in blank (tourmaline only and H_2O_2 only) and Fenton-like.

Fig. S2. Micrograph of aerobic activated sludge.